1-1-2015

Assessment of optimum width and longevity of a permeable reactive barrier installed in an acid sulfate soil terrain

Udeshini Pathirage
University of Wollongong, pp695@uowmail.edu.au

Buddhima Indraratna
University of Wollongong, indra@uow.edu.au

Assessment of optimum width and longevity of a permeable reactive barrier installed in an acid sulfate soil terrain

Abstract

Removal of contaminants from groundwater using permeable reactive barriers (PRBs) is a cost-effective and popular engineering solution used throughout the world. Dissolved pollutants in groundwater are removed through geochemical processes that make PRBs effective for different types of contaminants. In achieving this, it is vital to determine the optimum width of the PRB to allow adequate residence time within the barrier and to establish its longevity. For this purpose, both field monitoring and geochemical modelling were conducted for a trial PRB located in the Shoalhaven Floodplain, south of Wollongong in Australia. In this study, the optimum PRB width is evaluated numerically, based on the neutralization effectiveness, i.e., when acidic groundwater travels through the alkaline PRB. A model developed previously has been extended considering the residence time, reaction kinetics, mineral precipitation-induced reduction in porosity and hydraulic conductivity, influent concentrations of the contaminants, and groundwater flow velocity. Longevity of the PRB is determined with respect to groundwater flow rates and amount of reactive material consumed.

Disciplines

Engineering | Science and Technology Studies

Publication Details

Pathirage, U. & Indraratna, B. (2015). Assessment of optimum width and longevity of a permeable reactive barrier installed in an acid sulfate soil terrain. Canadian Geotechnical Journal, 52 (7), 999-1004.

Technical Note:
Assessment of optimum width and longevity of a Permeable Reactive Barrier installed in an acid sulfate soil terrain

Udeshini Pathirage, University of Wollongong, Northfields Avenue, Wollongong 2522, udeshini@uow.edu.au

Buddhima Indraratna, University of Wollongong, Northfields Avenue, Wollongong 2522, indra@uow.edu.au

Corresponding Author: Prof. Buddhima Indraratna

Abstract

Removal of contaminants from groundwater using permeable reactive barriers (PRB) is a cost-effective and popular engineering solution practiced throughout the world. Dissolved pollutants in groundwater are removed through geochemical processes which make PRBs effective for different types of contaminants. In achieving this, it is vital to determine the optimum width of the PRB to allow adequate residence time within the barrier and to establish its longevity. For this purpose, both field monitoring and geochemical modelling were conducted for a trial PRB located in the Shoalhaven Floodplain, South of Wollongong city in Australia. In this study, the optimum PRB width is evaluated numerically, based on the neutralisation effectiveness, i.e. when acidic groundwater travels through the alkaline PRB. A model developed previously has been extended considering the residence time, reaction kinetics, mineral precipitation induced reduction in porosity and hydraulic conductivity, the influent concentrations of the contaminants, and the groundwater flow velocity. The longevity of the PRB is determined with respect to the

groundwater flow rates and the amount of reactive material consumed.

Key words: Optimum width, permeable reactive barrier, acid sulfate soil.

Introduction

Permeable reactive barriers (PRB) have been recognised as versatile and promising engineering technology to treat contaminants dissolved in groundwater. Their increased popularity has been demonstrated in the remediation of contaminants, applied to acid mine drainage (Waybrant et al. 2002), and the removal of chlorinated organic compounds (Gillham and O'Hannesin 1994), and the removal of industrial waste (volatile organic compounds) (Vogan et al. 1999), as well as chromate, heavy metals and radionuclides (Ludwig et al. 2002). The remediation or neutralisation process occurs mainly through physical, chemical and/or biological means associated with mineral precipitation, sorption, and oxidation/reduction of ions (Rumer and Ryan 1995). There are some limitations associated with PRBs. The treatment zone of PRBs is restricted to shallow plumes, hence extending them for deep aquifers can be costly (Lehr 2004). Another drawback of PRBs is the potential clogging due to chemical and biological precipitates which may require timely maintenance or partial replacement of the reactive material. Zero valent iron (ZVI) PRBs used worldwide have endured clogging due to secondary mineral precipitation (Blowes et al. 2000, Li and Benson 2005). Moreover, the short-term capital cost for PRB construction and installation can be higher than that of pump-and-treat type approach (Lehr 2004).

The size of the PRB governs the residence time (i.e. time that the water is in contact with the reactive materials), which affects its longevity (Gavaskar et al. 1998). Nardo et al. (2010) presents a numerical methodology to an activated carbon PRB for the remediation of a tetrachloroethylene polluted aquifer, where the optimum width and position of the PRB was estimated considering groundwater flow velocities and first order reaction kinetics. Longevity of the PRB depends mainly on its chemical characteristics, which depend on the size of the PRB, including the total mass of reactive media and the rate of reactions (Blowes et al. 2000). Furthermore, it is important to consider the groundwater flow velocity through the barrier, and its porosity and hydraulic conductivity prior to construction. These hydraulic properties allow sufficient pore space for secondary minerals to precipitate and minimise the total clogging of the PRB (Gavaskar 1999).

Different types of alkaline materials have been used in PRBs for acidic groundwater remediation. Blowes et al. (2003) used organic carbon-rich materials such as wood chips, municipal compost and paper mill pulp to treat acidic groundwater generated from acid mine drainage (AMD). In this PRB, extensive precipitation of metal sulfides and bacterial residue hindered the reactivity of organic carbon-rich material (Blowes et al. 2003). Another AMD problem was maintained through a PRB consisting of limestone chips, compost, cattle slurry and pea gravel (Amos and Younger 2003), where the alkalinity generated from these materials was able to neutralise the acidity.

The performance of a limestone and red mud mixed PRB was discussed by Komnitsas et al. (2004) to treat AMD and toxic metals, whereby the neutralisation occurred through precipitation of heavy metals and sorption, as well as a reduction in longevity (Komnitsas et al. 2004).

This paper describes the determination of optimum width and longevity of a PRB in order to remediate the acidic groundwater generated at acid sulfate soil terrains in the Shoalhaven Floodplain. For this purpose, the original geochemical algorithm and groundwater flow model presented earlier by Indraratna et al. (2014) had to be extended, whereby MODFLOW and RT3D finite difference codes were employed as the numerical tools.

Theoretical Considerations and Background

The most important aspect when designing a PRB is that the residence time of the contaminated groundwater, should be long enough for the reaction process to occur. There have been several past studies carried out to optimise the barrier thickness or the width, in order to obtain the maximum usage of a PRB configuration. Elder et al. (2002) calculated the required thickness using a one-dimensional plug-flow model with first order reactions as given by:

$$b_{des} = \frac{-Ki}{k_r n} \ln\left(\frac{C_e}{C_{in}}\right) \qquad (1)$$

where, b_{des} is the design thickness of the PRB taken by applying a safety factor (SF), K is the hydraulic conductivity of the PRB, i is the hydraulic gradient, k_r is the first-order reaction rate constant, n is the porosity, C_e is the effluent concentration of the contaminant from the PRB and C_{in} is the influent contaminant concentration.

Considering the time-dependent performance of a PRB with respect to mineral fouling on reactive surfaces, as well as seasonal changes in the hydraulic gradient and direction of flow, Elder et al. (2002) used a SF of two. Hemsi and Shackelford (2006) discuss the SF associated with variable flow and aquifer heterogeneity in more detail. However, to account for the heterogeneity and/or anisotropy of some PRB materials, a SF as large as six has also been recommended (Eykholt 1997), thus,

$$SF = b_{des} / b_{cal} \qquad (2)$$

Fronczyk and Garbulewski (2010) computed the thickness of a PRB (b_{cal}) comprised of zeolite-sand mixture, using the following equation:

$$b_{cal} = \frac{t_{PRB} v_a}{R} \qquad (3)$$

where, b_{cal} is the calculated PRB thickness, v_a is the groundwater velocity, t_{PRB} is the working time and R is the retardation factor.

Fronczyk and Garbulewski (2010) introduced a critical hydraulic conductivity (k_{cr}), which was defined as the hydraulic conductivity of the aquifer ($k_s = k_g$) =

k_{cr}, where k_s and k_g were the hydraulic conductivities of the reactive medium and the aquifer, respectively.

Based on solid waste landfill pollution by tetrachloroethylene (PCE), Nardo et al. (2010) suggested that the optimum width of a PRB (b_{opt}) can be estimated using the following inequality:

$$\frac{b_{opt}}{u_b} \rangle \left(k_c a\right)^{-1} \tag{4}$$

where, u_b is the groundwater velocity inside the barrier, k_c is the total mass transfer coefficient for adsorption, and a is the external specific surface of the absorbent particles.

None of the above methods incorporated the effect of actual change in porosity and hydraulic conductivity due to the chemical reactions, when calculating the optimum width of a PRB. Therefore, it is imperative to develop a model which couples the groundwater flow, chemical reactions and associated reductions in porosity and hydraulic conductivity to accurately predict the optimum PRB width.

Proposed Numerical Methodology

There are mainly two contaminants, i.e. dissolved aluminium (Al^{3+}) and iron (Fe^{2+} and Fe^{3+}) associated with acidic groundwater generated within a typical

Australian acid sulfate soil terrain that contains a shallow layer of pyrite which oxidises in the presence of moisture to produce sulfuric acid. Acidic groundwater leaches out aluminium and iron from the soil into soluble ionic form. Al^{3+} is very toxic to fish and other aquatic species. Acid attacks on steel and concrete infrastructure, as well as unfavourable implications on aquaculture are well known (Indraratna et al. 2005). For instance, aluminium and iron deposit on the gills of fish causing fatalities (Dent and Pons 1995). The effects of other metals (Na^+, K^+, Mg^+) are not significant (Indraratna et al. 2014) when compared to the adverse effects attributed to high concentrations of aluminium and iron (Banasiak et al. 2014). In the current study, a PRB consisting of recycled concrete aggregates was installed at a local paddock in the Shoalhaven Floodplain about 65 km South of Wollongong City, Australia. One of the main factors influencing the optimum width of this PRB was the precipitation of aluminium and iron oxides/hydroxides (secondary minerals), and the corresponding chemical and geo-hydraulic characteristics of the groundwater flow. Indraratna et al. (2014) proposed a coupled hydro-geochemical model to simulate the transport of contaminants through the PRB, capturing the change in porosity (n) and hydraulic conductivity (K) due to mineral precipitation. Commercially available finite different codes MODFLOW and RT3D were used for this numerical analysis.

The reaction kinetics for precipitation of secondary minerals were calculated using the Transition State theory (Eqn. 5).

$$r = -k_r \left(1 - \frac{IAP}{k_{eq}} \right) \quad (5)$$

$$SI = \log(IAP) - \log(k_{eq}) \quad (6)$$

where, r is the reaction rate, k_r is the effective rate coefficient, IAP is the ion activity product, k_{eq} is the equilibrium solubility constant and SI is the saturation index. SIs can be calculated using PHREEQC software given the influent conditions. PHREEQC is a computer program for speciation, batch-reaction, one-dimensional transport and inverse geochemical calculations. For standalone clarity, the details of the geochemical algorithm previously discussed by Indraratna et al. (2014), which shows the relationship between the reaction rate for a substance (*r)* and the overall reaction rate for a specific ion (*R*)*,* are given in the Appendix. It shows all the chemical reactions associated with secondary mineral precipitation for aluminium and iron in their forms of oxides and hydroxides.

As MODFLOW does not automatically change the porosity and hydraulic conductivity due to secondary mineral precipitation, it was vital to update these values at each time step as captured in Eqns. 7 and 8.

$$\frac{\partial \phi_k}{\partial t} = M_k R_k \quad (7)$$

$$n_t = n_0 - \sum_{k=1}^{N_m} M_k R_k t \qquad (8)$$

where, ϕ_k is the volume fraction of precipitated mineral, M_k is the molar volume of mineral (m^3mol^{-1}) and R_k is the total reaction rate for a particular substance ($molm^{-3}_{bulk}s^{-1}$), N_m is the number of minerals and n_0 and n_t are the initial porosity and porosity at time t, respectively.

The normalised Kozeny Carmen equation (Eqn. 9) was then used to calculate the change in hydraulic conductivity (K) caused by mineral precipitation, hence,

$$K = K_0 \left[\frac{n_0 - \Delta n_t}{n_0}\right]^3 / \left[\frac{1 - n_0 + \Delta n_t}{1 - n_0}\right]^2 \qquad (9)$$

where, K_0 is the initial hydraulic conductivity and Δn_t is the difference in porosity at two consecutive time intervals.

MODFLOW iteratively calculates the pressure head based on the finite difference method (FDM) at each time step. For this pilot-scale PRB, the FDM simulation involved a discretised mesh of 1.2 m x 0.1 m along the centreline of the PRB with element (square plan area) spacing of 0.1 m (Figure 1). The piezometer locations at the entrance (P9) and exit (P8) of the PRB are shown in Figure 1, and the flow along the PRB centreline is considered as one-dimensional.

The pressure head solution (*h*) for transient groundwater flow in one-dimension is given by Eqn. 10, which was used in MODFLOW to calculate the initial head (close to P9) at each time step.

$$h = \left(\exp\left[-\frac{\mu^2 B K_0}{S \sum_{k=1}^{N_m} M_k R_k} \frac{(1-n_0)^2}{n_0^3} \left\{ \alpha^2 \left(1.5 + \frac{1}{\beta} \right) - 3(\alpha + \ln\beta) \right\} \right] \right) \cdot (C \sin \mu x + D \cos \mu x) \quad (10)$$

In the above, *B* is the aquifer thickness, *S* is the storage co-efficient, *μ, C* and *D* are constants. The parameters *α* and *β* are given by:

$$\alpha = n_0 + \sum_{k=1}^{N_m} M_k R_k t \quad (10a)$$

$$\beta = 1 - n_0 - \sum_{k=1}^{N_m} M_k R_k t \quad (10b)$$

RT3D solves coupled partial differential equations which describe reactive flow and transport of multiple species in saturated groundwater systems, as represented by Eqn. 11. In fact, RT3D has seven pre-programmed reaction modules plus the capability to accommodate user-defined options, and these can be used to simulate different types of reactive contaminants for a given contaminant transport problem. In this study, the user-defined module was adopted, whereby the specifically developed geochemical algorithm (details in Appendix) was incorporated through the reaction component ($R_k M_k C$) in

Eqn.11.

$$R_e \frac{\partial C}{\partial t} = D\frac{\partial^2 [C]}{\partial x^2} - u_b \frac{\partial [C]}{\partial x} - R_k M_k C \qquad (11)$$

where, C is the concentration of the contaminant, R_e is the retardation coefficient, D is the dispersion coefficient.

As an example, when the numerical simulation was carried out for the first time step, the resulting head at the PRB exit (near P8) was obtained based on the Runge-Kutta iteration method. RT3D could then receive the head solution from MODFLOW as input, and the groundwater flow velocity (u_b) was subsequently calculated using Eqn. 12 for that particular time step, thus,

$$u_b = -\frac{K}{n}\frac{\partial h}{\partial x} \qquad (12)$$

Subsequently, both MODFLOW and RT3D were run in conjunction to determine the contaminant transport characteristics of the selected species at each time step.

For the next time step a new value of R_k is determined from Eqns. 5 and 6, following the same geochemical algorithm (Appendix) and the RT3D output concentrations obtained from the previous time step. Subsequently, the corresponding porosity and hydraulic conductivity for the next time step are calculated using Eqns. 8 and 9, respectively. Using Eqn. 10, the initial head for the next time step is then calculated and incorporated in MODFLOW to

obtain the corresponding u_b as an input to RT3D. The above procedure was repeated in RT3D for consecutive time steps.

The iterative simulation carried out to determine the optimum width of PRB is illustrated in the flowchart shown in Figure 2. MODFLOW simulation was carried out after feeding the input data including K, n, h (initial hydraulic head from Eqn. 10). The next step was the RT3D simulation to compute the effluent concentration of the pollutants, $C_e\ (x,t)$. When C_e is lower than an acceptable limit (C_{lim}), the computed PRB width is considered to be sufficient, otherwise it must be increased until $C_e < C_{lim}$. The values of C_{lim} can be obtained from the Australian Water Guidelines (Sundaram et al. 2009), where the specific values of C_{lim} for both Al and Fe were 0.2 mg/L. All the values for model parameters are listed in Table 1. These values were obtained for a real-life PRB installed in the Lower Shoalhaven Floodplain, South of Wollongong, Australia. Therefore, these parameters are directly linked to the actual field condition. Moreover, the model calibration and validation for field conditions is elaborated by Indraratna et al. (2014). In fact, this technical note is an extension of the same project to optimise the width of the PRB. The field conditions are captured in this paper appropriately. For instance, a range of possible concentrations for influent Al and Fe existing in the field are used in this analysis to determine the optimum width of the PRB (Figure 3).

In the current analysis, the use of Eqns. 5 - 12 enables one to capture the effect of secondary mineral precipitation for calculating the optimum PRB width. However, it is also important to consider the influent concentrations which can fluctuate due to seasonal changes. Therefore, the PRB must be capable of catering for both extreme concentration peaks while sustaining an acceptable long-term performance. In view of the above, four possible concentrations of contaminants were compared as elaborated below.

Results

Results shown in Figure 3 imply that the optimum width of the PRB to be 0.45 m for a range of influent concentrations varying from 50 to 250 mg/L. A minimum SF of two has been suggested by Gavaskar (1998) and Nardo et al. (2010) to account for the inhomogeneity of PRB material across its width. Accordingly, the design width of PRB, after applying a SF of two would be 0.9 m. The pilot-scale PRB installed at Nowra had a width of 1.2 m (i.e. SF = 2.7), which is conservative for the remediation of acidic groundwater using recycled concrete aggregates.

Prediction of Longevity

The longevity of a typical PRB depends mainly on the exhaustion rate of reactive material and the precipitation rate of secondary minerals. The

continuous secondary mineral precipitation over time would decrease the effectiveness of the PRB, because they clog the reactive surfaces of recycled concrete particles and consequently reduce the acid neutralisation capacity (ANC). The column experiments carried out by Pathirage (2014) revealed that the reduction in ANC due to secondary mineral precipitation was 54%. Moreover, the piezometric heads (m AHD - Australian height datum) obtained for past six years inside the PRB were generally steady (Figure 4), which indicate that there is no significant threat of clogging from the precipitation of secondary minerals. This clearly implies that the only profound threat for long-term performance of the PRB would be the exhaustion of reactive material due to acid neutralisation and armouring of the reactive surfaces by secondary minerals which reduce the ANC. As this pilot-scale PRB contained 80 tonnes of recycled concrete attributing to an ANC of 146 g/kg, at least 11.7 tonnes of acid neutralisation capacity was expected to be available in this PRB. The groundwater velocity at this field site typically fluctuates from 0.01-0.1 m/day. Assuming a mean groundwater flow velocity of 0.05 m/day and considering the initial PRB porosity of approximately 50% (void ratio close to unity), acid transported through the PRB was determined to be 4.85×10^5 L/year. The averaged acidity at the study site from September 2010 to July 2012 was 565 mg/L (equivalent to $CaCO_3$), with a corresponding consumption of reactive material of 0.274 t/year. Therefore, in order to consume all the capable acid neutralising material, it would take 42.7 years ignoring the effect of armouring by

secondary minerals precipitation. When the effect of secondary minerals precipitation on ANC was incorporated, (i.e. 54%), the estimated longevity of the PRB would be at least 19.5 years for a mean groundwater velocity of 0.05 m/day. Naturally, the computed longevity would vary according to the groundwater flow velocity and the respective consumption of reactive material as plotted in Figure 5.

Conclusion

MODFLOW and RT3D finite difference codes were used to simulate the optimum width of a PRB installed at the Shoalhaven Floodplain, located on the Eastern coast of Australia. In order to satisfy the seasonal changes, the model was run for four different influent contaminant concentrations until the inequality, $C_e < C_{lim}$ was satisfied (i.e. when the effluent concentration (C_e) becomes lower than an acceptable limit value (C_{lim})). Incorporating a recommended safety factor of 2, the optimum design width of the PRB was determined to be 0.9 m based on the numerical simulations. Therefore, the current pilot-scale PRB having a width of 1.2 m, can be regarded as conservative for the remediation of acidic groundwater using recycled concrete aggregates. The predicted longevity of the PRB considering the effect of armouring due to secondary mineral precipitation was at least 19.5 years for a mean groundwater flow velocity of 0.05 m/day.

Acknowledgement

Authors are grateful for funding received from the Australian Research Council (ARC) and industry partners Southern Rivers Catchment Management Authority (SRCMA), Douglas Partners Pty Ltd. and Manildra Group. The assistance given to Authors at various times by Glenys Lugg, Dr. Laura Banasiak and Dr. Gyanendra Regmi are gratefully appreciated. The authors acknowledge technical staff at the University of Wollongong especially Bob Rowlan and Frank Crabtree for their assistance in field monitoring. Authors acknowledge Elsevier Publication for allowing permission to re-use some of technical content published in Computers and Geotechnics.

References:

Amos, P.W., and Younger, P.L. 2003. Substrate characterisation for a subsurface reactive barrier to treat colliery spoil leachate. Water Research, **37**: 108-120.

Banasiak, L.J., Indraratna, B., Lugg, G., Pathirage, U., Mcintosh, G., and Rendell, N. 2014. Permeable reactive barrier rejuvenation by alkaline wastewater. Available from: http://www.icevirtuallibrary.com/content/article/10.1680/envgeo.13.00122.

Blowes, D.W., Ptacek, C.J., Benner, S.G., Mcrae, C.W.T., Bennett, T.A., and Puls, R.W. 2000. Treatment of inorganic contaminants using permeable reactive barriers. Journal of Contaminant Hydrology, **45**: 123-137.

Blowes, D.W., Ptacek, C.J., Jambor, J.L., and Weisener, C.G. 2003. The Geochemistry of Acid Mine Drainage. *In* Treatise on Geochemistry. *Edited by* H.D. Holland and K.K. Turekian. Oxford: Elsevier Science Ltd. pp 149-204.

Dent, D.L., and Pons, L.J. 1995. A world perspective on acid sulphate soils. Geoderma, **67**: 263-276.

Elder, C.R., Benson, C.H., and Eykholt, G.R. 2002. Effects of heterogeneity on influent and effluent concentrations from horizontal permeable reactive barriers. Water Resources Research, **38**: 27-1-27-19.

Eykholt, G. 1997. Uncertainty based scaling of iron reactive barriers. *In* Proceedings of the In Situ Remediation of the Geoenvironment. American Society of Civil Engineers, New York, pp. 41-45

Fronczyk, J., and Garbulewski, K. 2010. Design Procedure for Permeable Reactive Barrier with Zeolite-sand Maixture. *In* Proceedings of the 6th International Congress on Environmental Geotechnics, New Delhi, India, pp. 777-781.

Gavaskar, A.R., Gupta, N., Sass, B.M., Janosy, R.J., and O'sullivan, D. 1998. Permeable Barriers for Groundwater Remediation: Design, Construction, and Monitoring, Columbus, Battelle Press.

Gavaskar, A. R. 1999. Design and construction techniques for permeable reactive barriers. Journal of Hazardous Materials, **68**: 41-71.

Gillham, R.W., and O'hannesin, S.F. 1994. Enhanced degradation of halogenated aliphatics by zero-valent iron. Ground Water, **32**: 958-967.

Hemsi, P. S. and Shackelford, C. D. 2006. An evaluation of the influence of aquifer heterogeneity on permeable reactive barrier design. Water Resources Research, **42**: W03402.

Indraratna, B., Golab, A., Glamore, W., and Blunden, B. 2005. Acid sulphate soil remediation techniques on the Shoalhaven River Floodplain, Australia. Quarterly Journal of Engineering Geology and Hydrogeology, **38**: 129-142.

Indraratna, B., Pathirage, P.U., Kerry, R.,a nd Banasiak, L. 2014. Coupled hydro-geochemical modelling of a permeable reactive barrier for treating acidic groundwater. Computers and Geotechnics Journal*,* **55**: 429-439.

Komnitsas, K., Bartzas, G., and Paspaliaris, I. 2004. Efficiency of limestone and red mud barriers: laboratory column studies. Minerals Engineering, **17**: 183-194.

Lehr, J.H. 2004. Wiley's RemediationaTechnologies Handbook: Major Contaminant Chemicals and Chemical Groups. John Wiley and Sons, Inc., New Jersey.

Li, L., Benson, C.H., and Lawson, E.L. 2005. Impact of mineral fouling on hydraulic behaviour of permeable reactive barriers. Ground Water, **43**(4): 582-596.

Ludwig, R.D., Mcgregor, R.G., Blowes, D.W., Benner, S.G., and Mountjoy, K. 2002. A permeable reactive barrier for treatment of heavy metals. Ground Water*,* **40**: 59-66.

Nardo, A.D., Natale, M.D., Erto, A., Musmarra, D., and Bortonea, I. 2010. Permeable reactive barrier for groundwater PCE remediation: the case study of a solid waste landfill pollution. *In* Computer Aided Chemical Engineering. *Edited by* S. Pierucci and G.B. Ferraris. Elsevier. Pp. 1015-1020.

Pathirage, U. 2014. Modelling of clogging in a permeable reactive barrier in acid sulfate soil terrain. PhD thesis, School of Civil, Mining and Environmental Engineering, University of Wollongong.

Pathirage, P. U. and Indraratna, B. 2014. Hydro-geochemical Model for Treating Acidic Groundwater using a Permeable Reactive Barrier. *In:* Proceedings of the 5th International Conference on Computational Methods. *Edited by* G. R. Liu and Z. W. Guan. 28–30 July 2014. ScienTech Publisher, Cambridge.

Regmi, G. 2012. Performance Validation of a Permeable Reactive Barrier (PRB) for Treating Acidic Groundwater. Degree of Doctor of Philosophy, University of Wollongong.

Rumer, R.R., and Ryan, M.E. 1995. Barrier Containment Technologies for Environmental Remediation Applications. John Wiley and Sons, New York.

Sundaram, B., Feitz, A.J., De Caritat, P., Plazinska, A., Brodie, R.S., Coram, J., and Ransley, T. 2009. Groundwater Sampling and Analysis - A Field Guild. Australia.

Vogan, J.L., Focht, R.M., Clark, D.K., and Graham, S.L. 1999. Performance evaluation of a permeable reactive barrier for remediation of dissolved chlorinated solvents in groundwater. Journal of Hazardous Materials, **68**: 97-108.

Waybrant, K.R., Ptacek, C.J., and Blowes, D.W. 2002. Treatment of mine drainage using permeable reactive barriers: column experiments. Environmental Science and Technology*,* **36**: 1349-1356.

Appendix:

Geochemical algorithm for secondary mineral precipitation

Transition state theory was applied to all chemical reactions as given in following expressions;

$$r = -k_r\left(1 - \frac{IAP}{k_{eq}}\right)$$

$$Fe^{3+} + 3H_2O \rightarrow Fe(OH)_{3(S)} + 3H^{+}_{aq}$$

$$\frac{d\left[Fe^{3+}\right]}{dt} = -\frac{d\left[m_{Fe(OH)_3}\right]}{dt} = -\frac{1}{3}\frac{d\left[H^+\right]}{dt} = r_{1\left[Fe^{3+}\right]} = k_{\left[Fe^{3+}\right]}\left[\frac{a_{Fe^{3+}}a^3_{OH^-}}{k_{eq,Fe^{3+},OH^-}} - 1\right]$$

$$Fe^{3+} + 2H_2O \rightarrow Fe(OOH) + 3H^{+}_{aq}$$

$$\frac{d\left[Fe^{3+}\right]}{dt} = -\frac{d\left[m_{Fe(OOH)}\right]}{dt} = -\frac{1}{3}\frac{d\left[H^+\right]}{dt} = r_{2\left[Fe^{3+}\right]} = k_{\left[Fe^{3+}\right]}\left[\frac{a_{Fe^{3+}}a_{OOH^{3-}}}{k_{eq,Fe^{3+},OOH^{3-}}} - 1\right]$$

$$2Fe^{3+} + 3H_2O \rightarrow Fe_2O_3 + 6H^{+}_{aq}$$

$$\frac{1}{2}\frac{d\left[Fe^{3+}\right]}{dt} = -\frac{d\left[m_{Fe_2O_3}\right]}{dt} = -\frac{1}{6}\frac{d\left[H^+\right]}{dt} = r_{3\left[Fe^{3+}\right]} = k_{\left[Fe^{3+}\right]}\left[\frac{a^2_{Fe^{3+}}a^3_{O^{2-}}}{k_{eq,Fe^{3+},O^{2-}}} - 1\right]$$

$$Al^{3+} + 3H_2O \rightarrow Al(OH)_{3(S)} + 3H^{+}{}_{(aq)}$$

$$\frac{d\left[Al^{3+}\right]}{dt} = -\frac{d\left[m_{Al(OH)_3}\right]}{dt} = -\frac{1}{3}\frac{d\left[H^+\right]}{dt} = r_{\left[Al^{3+}\right]} = k_{\left[Al^{3+}\right]}\left[\frac{a_{Al^{3+}}a^3_{OH^-}}{k_{eq,Al^{3+},OH^-}} - 1\right]$$

$$Fe^{2+} + 2(OH)^{-} \leftrightarrow Fe(OH)_{2(S)}$$

$$\frac{d\left[Fe^{2+}\right]}{dt}=\frac{1}{2}\frac{d\left[OH^{-}\right]}{dt}=-\frac{d\left[m_{Fe(OH)_2}\right]}{dt}=r_{1\left[Fe^{2+}\right]}=k_{\left[Fe^{2+}\right]}\left[\frac{a_{Fe^{2+}}a_{OH^{-}}^{2}}{k_{eq,Fe^{2+},OH^{-}}}-1\right]$$

$$Fe^{2+}+CO_3^{2-}\leftrightarrow FeCO_{3(S)}$$

$$\frac{d\left[Fe^{2+}\right]}{dt}=\frac{d\left[CO_3^{2-}\right]}{dt}=-\frac{d\left[m_{FeCO_3}\right]}{dt}=r_{2\left[Fe^{2+}\right]}=k_{\left[Fe^{2+}\right]}\left[\frac{a_{Fe^{2+}}a_{CO_3^{2-}}}{k_{eq,Fe^{2+},CO_3^{2-}}}-1\right]$$

The overall reactive kinetics for each species in the algorithm are listed as:

$$\frac{d\left[Fe^{3+}\right]}{dt}=r_{1\left[Fe^{3+}\right]}+r_{2\left[Fe^{3+}\right]}+2r_{3\left[Fe^{3+}\right]}=R_1$$

$$\frac{d\left[Fe^{2+}\right]}{dt}=r_{1\left[Fe^{2+}\right]}+r_{2\left[Fe^{2+}\right]}=R_2$$

$$\frac{d\left[Al^{3+}\right]}{dt}=r_{\left[Al^{3+}\right]}=R_3$$

Table Captions

Table 1 Parameters and values used in the model

Figure Captions

Figure 1 Discretisation of the centreline of PRB (not to scale)

Figure 2 Flow chart of the optimum PRB width determination process

Figure 3 Effluent concentrations vs. PRB width (b_{opt}) for different influent concentrations

Figure 4 Groundwater elevations inside the PRB with respect to time (P7-P12 are the six piezometers inside the PRB) (after Pathirage and Indraratna (2014), (data updated after Regmi (2012)))

Figure 5 Longevity of the PRB with respect to groundwater velocity and consumption of reactive material

Table 1 Parameters and values used in the model

Parameter	Value
k_r of Ca^{2+} (mol/L.s)[a]	2.27×10^{-7}
k_r of Al^{3+} (mol/L.s)[a]	6.86×10^{-8}
k_r of Total Fe (Fe^{2+} and Fe^{3+}) (mol/L.s)[a]	5.87×10^{-8}
Longitudinal dispersivity (m)	0.3
Retardation coefficient (R_e)	1
Initial porosity (n_0) of the PRB	0.5
Initial hydraulic conductivity (K_0) (ms^{-1})	0.1
Mean groundwater flow velocity (m/day)	0.05

[a](Indraratna et al. 2014)

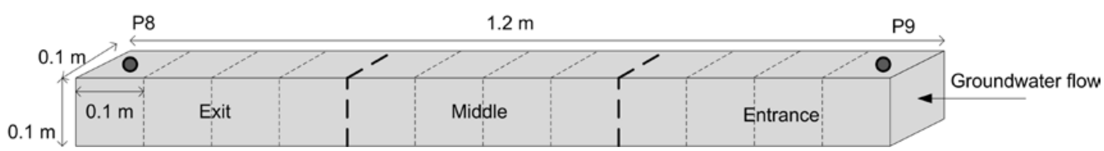

Figure 1 Discretisation of the centreline of PRB (not to scale)

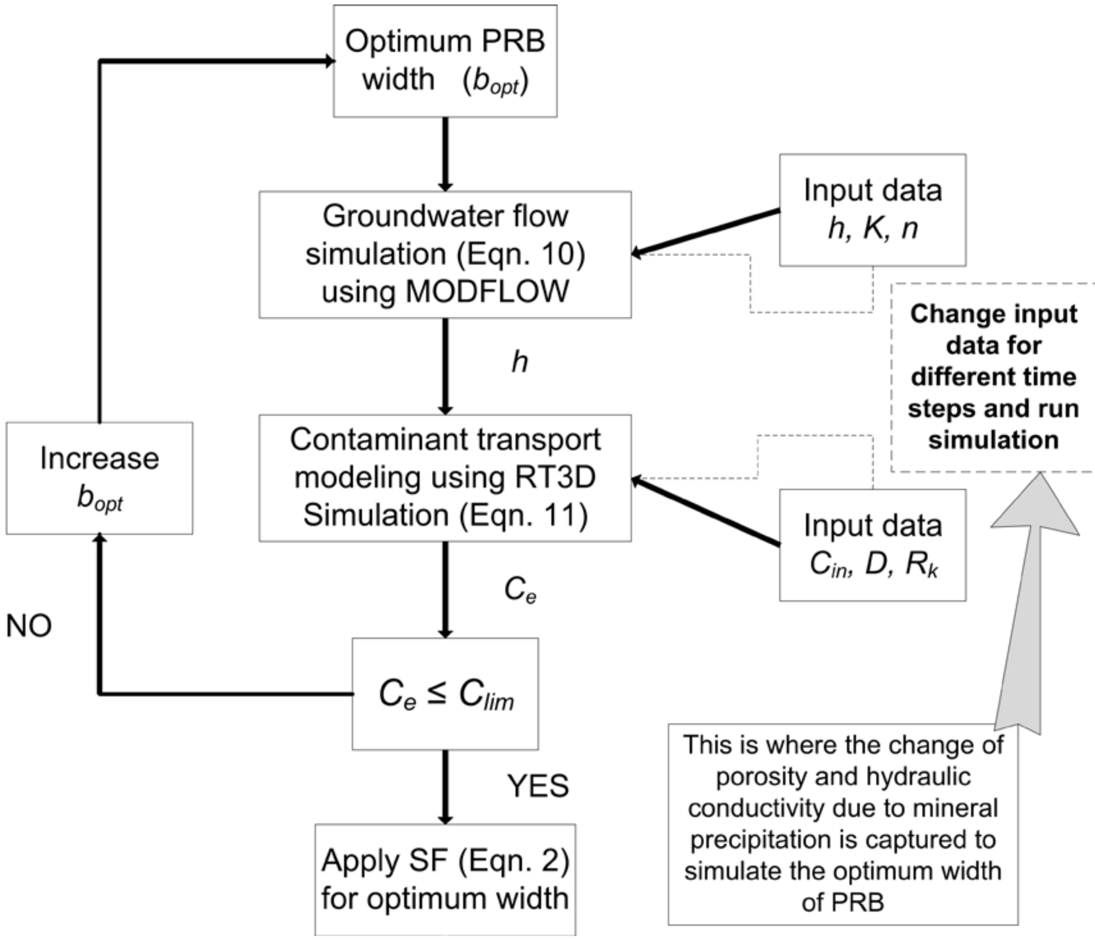

Figure 2 Flow chart of the optimum PRB width determination process

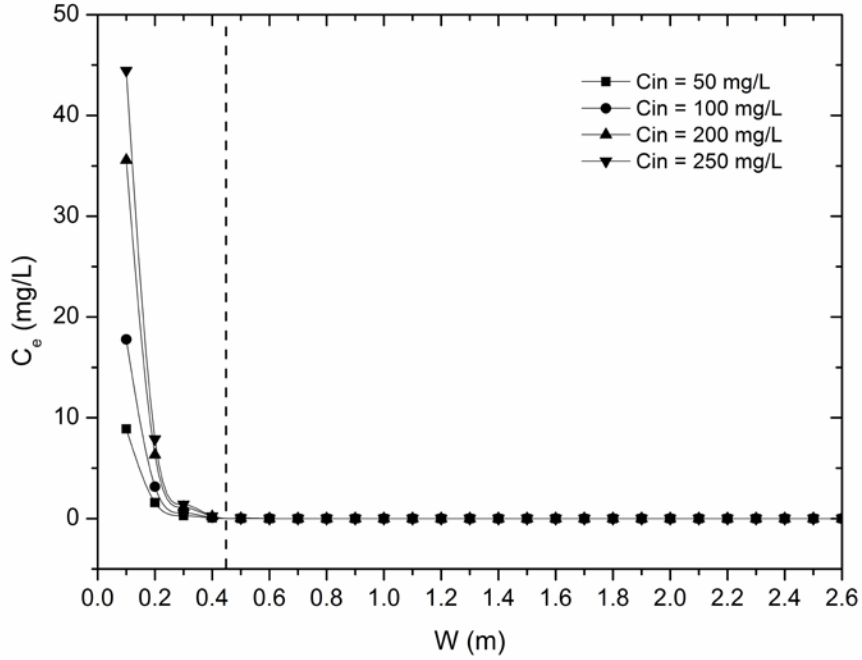

Figure 3 Effluent concentrations vs. PRB width (b_{opt}) for different influent concentrations

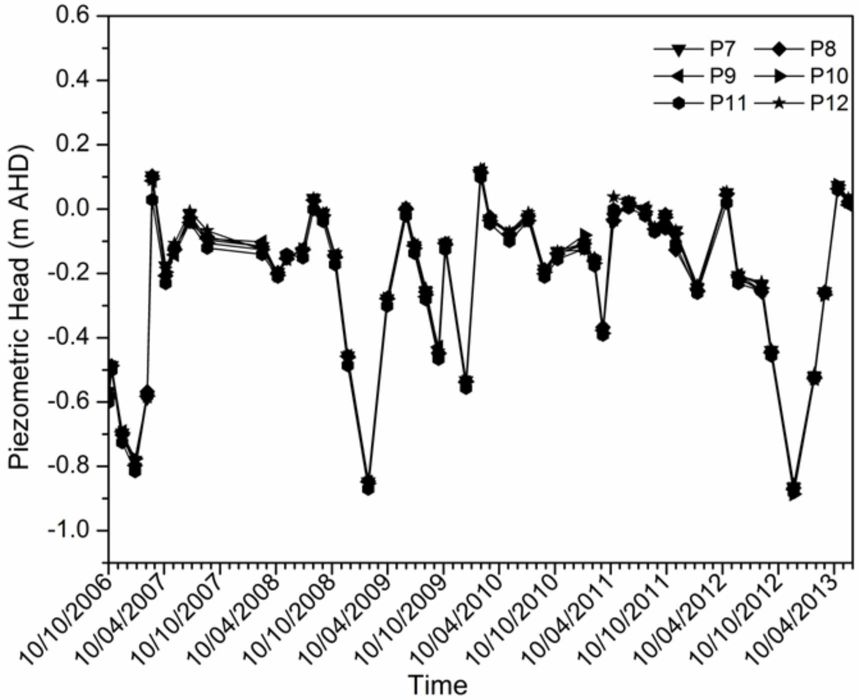

Figure 4 Groundwater elevations inside the PRB with respect to time (P7-P12 are the six piezometers inside the PRB) (after Pathirage and Indraratna (2014), (data updated after Regmi (2012)))

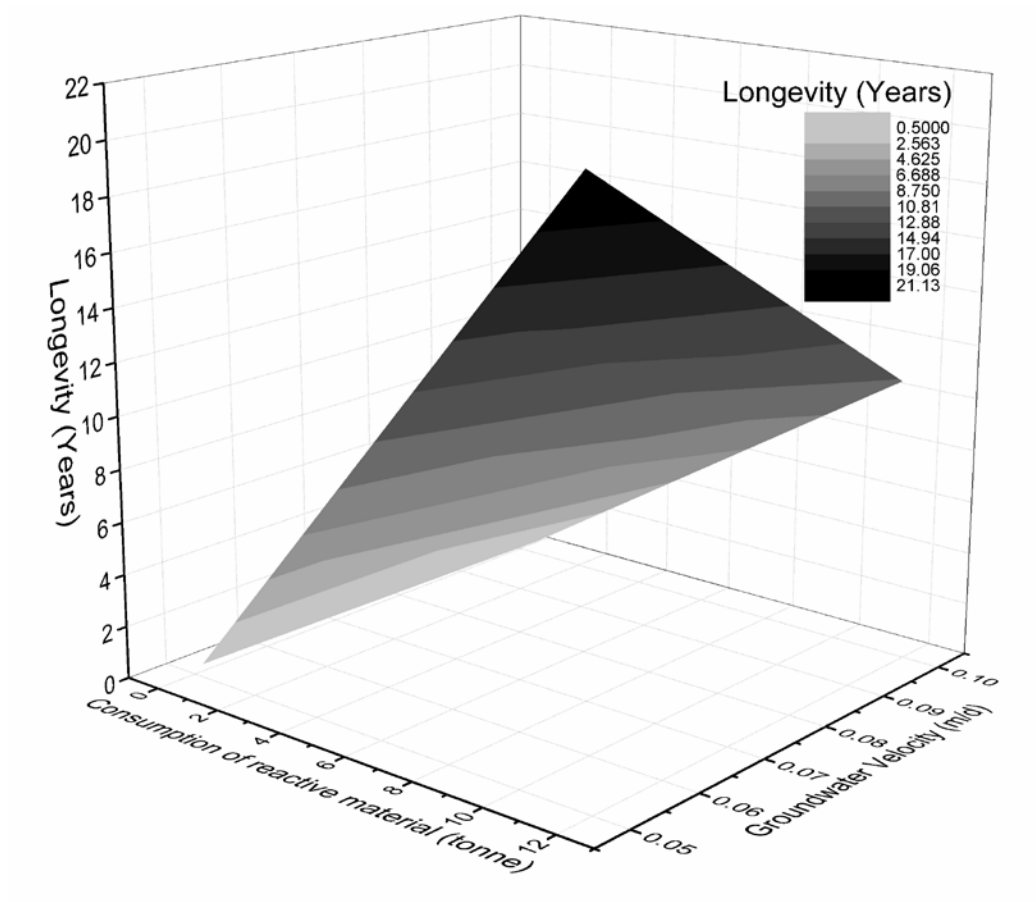

Figure 5 Longevity of the PRB with respect to groundwater velocity and consumption of reactive material